An Nbody Integrator for Planetary Rings

Joseph M. Hahn
Space Science Institute
Austin, TX

Carolyn Porco
CICLOPS/SSI
Boulder, CO

Joseph Spitale
CICLOPS/SSI
Tucson, AZ

Introduction

Although Nbody methods are widely used to study disk-planet interactions, such methods are difficult to apply in a planetary ring. This is because the ring's highly organized response to satellite perturbations (eg, a spiral density wave, or a scalloped ring-edge) has small forced eccentricities $e \lesssim 10^{-4}$. In an Nbody simulation, the ring's gentle collective motions are easily swamped by gravitational scattering among the system's finite number of particles. Although this difficulty is avoided in simulations of a small patch of many low-mass particles (Salo 1995, Salo et al 2001), the patch method cannot be used to model large-scale disturbances in a ring.

Alternatively, fluid dynamics can be used to study a perturbed ring's collective behavior. The planetary ring is treated as a collection of streamlines that interact via gravity and hydrodynamic forces. This results in a coupled system of nonlinear differential equations that are solved for the ring's equilibrium state (Borderies et al 1985, 1989, Hahn et al 2009). However these equations' considerable complexity might explain why this method is not widely used to calculate a ring's evolution over time.

To address this, the following describes an algorithm that combines Nbody methods with streamline dynamics, resulting in a code that calculates the ring's time evolution. The code is then used to model two systems: the scalloped edge of Saturn's B ring, and a nonlinear density wave.

Numerical method

A 2^{nd} order Wisdom-Holman map advances the particles in time (Wisdom & Holman 1991, Saha & Tremaine 1992). This kick-drift scheme has orbit elements 'kicked' by the perturbing forces during timestep Δt, plus an unperturbed orbital 'drift' during Δt. Motion around an oblate planet is epicyclic, so particle coordinates are $r = a(1-e\cos M)$ and $\theta = \tilde{\omega} + M + 2e\sin M$ where the orbit elements $a, e, M, \tilde{\omega}$ experience kicks

$$\Delta a = \left\langle \left[A_r e\sin M + A_\theta \frac{\Omega}{\kappa}(1+e\cos M) \right] \frac{2\Delta t}{\kappa} \right\rangle \quad \text{and} \quad \Delta e = \left[A_r \sin M + A_\theta \frac{2\Omega}{\kappa}\cos M \right] \frac{\Delta t}{a\kappa}, \tag{1}$$

$$\Delta\tilde{\omega} = -\left[A_r \cos M - A_\theta \frac{2\Omega}{\kappa}\sin M \right] \frac{\Delta t}{ea\kappa} \quad \text{and} \quad \Delta M = \left[A_r \cos M - A_\theta \frac{2\Omega}{\kappa}\sin M \right] \frac{\Delta t}{ea\kappa}, \tag{2}$$

every timestep Δt due to the radial and azimuthal accelerations A_r, A_θ, while the unperturbed motion drifts as $\Delta\tilde{\omega} = (\Omega - \kappa)\Delta t$ and $\Delta M = \kappa \Delta t$ (from Longaretti & Borderies 1991, to $O(e)$). The Δa's are also orbit-averaged so that all particles on a streamline maintain a common semimajor axis a over time. Torques are also applied to the inner and outer streamlines to prevent any viscous radial spreading of the ring.

Streamlines, and the ring's internal forces

A streamline is the path traced by numerous ring particles having a common semimajor axis a; see Fig. 1. The streamline concept is a very useful here, because the forces that a streamline exerts on a particle (gravity, pressure, etc) are simple functions of separation Δr. These streamlines are also in close proximity, so a particle will sense a nearby streamline as a long straight wire of linear density λ. Consequently, the surface density at any site is simply $\sigma = \lambda/\Delta r$, while the gravitational acceleration from a streamline is $A_r = 2G\lambda/\Delta r$. Some models also use a fictitious drag acceleration $\mathbf{A} = -C_d \Omega \Delta \mathbf{v}$ where $\Delta\mathbf{v}$ is the particle's velocity relative to the circular speed, and C_d is the drag coefficient; this force can prevent the ring from getting so disturbed that streamlines cross, which is problematic.

Compressible ring: Most of the simulations here assume that the ring is compressible with pressure $p = c^2\sigma$. In this case, the acceleration due to ring pressure is $A_r = -(c^2/\sigma)(\partial\sigma/\partial r)$, while that due to ring viscosity is

$$A_r = \left(\frac{4}{3}\nu_s + \nu_b\right)\frac{1}{\sigma}\frac{\partial}{\partial r}\left(\sigma\frac{\partial v_r}{\partial r}\right) \quad \text{and} \quad A_\theta = \frac{\nu_s}{\sigma}\frac{\partial}{\partial r}\left(\sigma\frac{\partial v_\theta}{\partial r}\right). \tag{3}$$

where ν_s, ν_b are the ring's kinematic shear and bulk viscosities, and v_r, v_θ are the particles' radial and tangential velocities.

Incompressible ring: We also consider an incompressible ring whose particles are packed shoulder to shoulder. Any horizontal compression of the ring then increases the ring's vertical thickness h, which is related to the surface density via $h = \sigma/2\rho$ where ρ is the ring's constant volume density. The vertical component of the planet's gravity also pushes ring-matter to the midplane, resulting in pressure $p = \rho(h\Omega)^2/3 = (\sigma\Omega)^2/12\rho$. For isotropic pressure, this results in acceleration $A_r = -\rho^{-1}(\partial p/\partial r)$, while the viscous acceleration is similar to Eqn. (3) but with $\nu_b = 0$ and $4/3 \to 1$.

Acknowledgments:
Support to JMH is provided by NASA's Outer Planets Research Program.

Simulations of the B ring's outer edge

The B ring's outer edge is controlled by an $m = 2$ inner Lindblad resonance with the satellite Mimas, with the ring-edge lying 14 km exterior to this resonance (Spitale & Porco 2010). As expected, the B ring-edge has an m=2 component with an epicyclic amplitude of R=35 km, which trails Mimas by by $\phi = -3^\circ$ (Spitale & Porco 2010). Cassini observations also show that the ring-edge has $m = 1$ and $m = 3$ disturbances there, as well as a freely precessing $m = 2$ component, but these disturbances are not yet accounted for by this model, and are not considered further here.

Drag-dominated ring: Figure 1 shows a simulated B ring after it settles to equilibrium at time $t = 50$ yrs or 4×10^4 orbits. Dots indicate particle positions, and curves connect particles along streamlines. A compressible equation of state is used here, and dissipation due to a fictitious drag having $C_d = 3 \times 10^{-5}$ causes the ring's $m = 2$ pattern to lap behind Mimas by $\phi = -5^\circ$. A ring having a higher surface density will have a smaller epicyclic amplitude R, and this simulated ring's surface density $\sigma_0 = 100$ gm/cm^2 was chosen to match the B ring's observed amplitude $R = 35$ km.

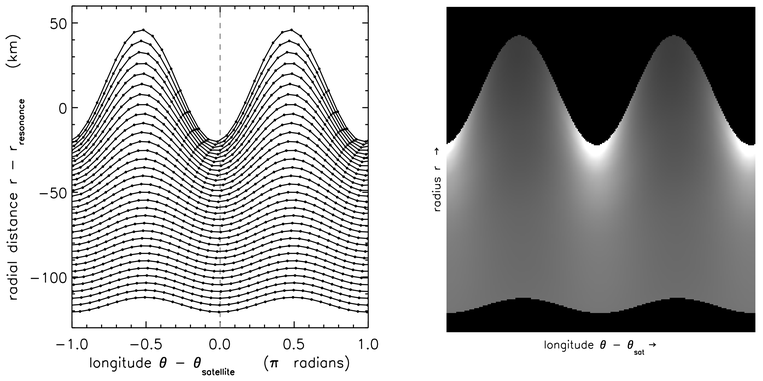

FIGURE 1: The outer B ring's response to Mimas' $m = 2$ ILR. This simulation uses $N_p = 32$ particles (dots) in $N_s = 32$ streamlines (curves), with $NpNs = 1$k total. Greyscale shows the ring's surface density varies over $0.5 > \Delta\sigma/\sigma > 2$. The model assumes ring surface density $\sigma_0 = 100$ gm/cm^2, a compressible EOS with c chosen so Toomre's stability parameter $Q = 2$, and dissipation due to drag with $C_d = 3 \times 10^{-5}$.

Viscosity-dominated ring: Figure 2 shows a more realistic simulation where dissipation in the ring is due to viscous friction that accounts for other unmodeled effects, such as collisions or scattering among particles. A rather heavy viscosity, $\nu_s = 600$ cm^2/sec and $\nu_b = 3\nu_s$, is used to make the ring's $m = 2$ pattern lag behind Mimas' longitude by $\phi = -5^\circ$. Note also the banded pattern in the ring's surface density, which is due to alternating separations among adjacent streamlines. This banding is only seen when dissipation in the ring is dominated by viscosity, which suggests that this effect might be associated with viscous overstability. Note also that this banding is most prominent at the ring's outer edge, which is most strongly disturbed by Mimas $m = 2$ ILR. The bands' radial spacing is $\Delta r \sim 10$km in these simulations, but this only an upper limit because ongoing higher-resolution simulations show similar banding on smaller scales.

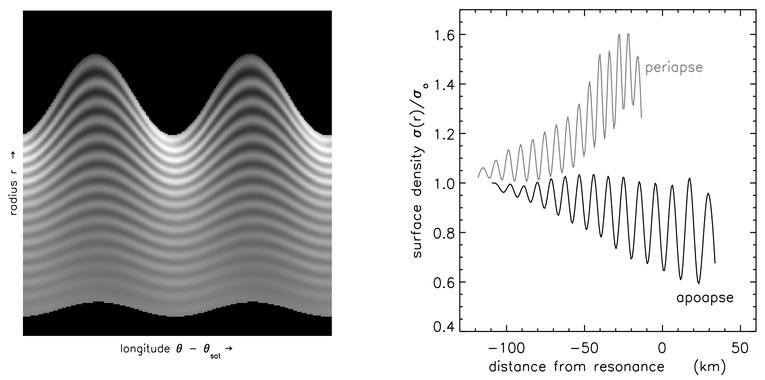

FIGURE 2: Dissipation in this simulated B ring is due shear viscosity $\nu_s = 600$ cm^2/sec and bulk viscosity $\nu_b = 3\nu_s$. Undisturbed ring surface density is $\sigma_0 = 165$ gm/cm^2, and compressible EOS with $Q = 2$ is used. Right figure shows radials surface density variations along ring's longitude of periapse and apoapse.

Incompressible ring: Figure 3 considers a B ring whose particles are so close-packed that they obey the incompressible equation of state. This ring is much more dynamic, and does not settle down to steady state. Rather, this ring experiences $m = 2$ spiral density waves that propagate both inwards and outwards. Waves reflect at ring-edges and superimpose at ring center, causing large fluctuations in surface density. Eventually the ring gets so disturbed that streamlines cross and subsequent evolution is unreliable; Fig. 3 shows the ring just before then. Surface density variations also cause variations in the ring's vertical thickness $h = \sigma/2\rho$, shown as radial cuts along the ring's longitude of periapse and apoapse.

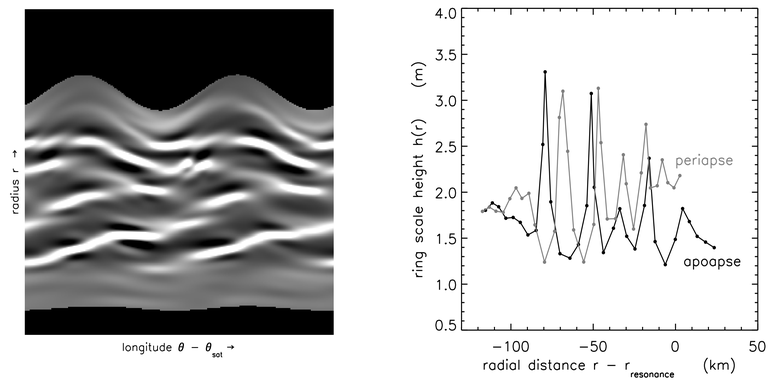

FIGURE 3: Simulation of incompressible B ring at time $t = 2.7$ yrs (2000 orbits), just before streamlines in the disturbed region cross. This ring has undisturbed surface density $\sigma_0 = 180$ gm/cm^2, viscosity $\nu_s = 600$ cm^2/sec and $\nu_b = 3\nu_s$, undisturbed scale height $h_0 = 1.8$m, and constant volume density $\rho = 0.5$ gm/cm^3. Right figure shows scale height $h = \sigma/2\rho$ along the ring's longitude of periapse and apoapse.

Note that the outcome seen in Fig. 3 might be a consequence of boundary conditions, which treats the simulated ring's inner and outer streamlines as hard edges. Consequently, spiral waves do not escape the simulation, which may be why the ring does not settle to equilibrium. This will be examined closely as we implement a radiative boundary condition that allows inward-propagating waves to escape. Lastly, note that this model does not yet account for the ring's vertical gravity, which will increase ring pressure and, we suspect, cause spiral waves to propagate even faster.

Spiral density waves

Figure 4 demonstrates that the code developed here can also simulate nonlinear spiral density waves launched at a satellite's m^{th} Lindblad resonance. This simulation of an $m = 2$ spiral used 1.5k particles, and was evolved for 5000 orbits, which is the time for this wave to propagate about six wavelengths. Execution time on a desktop PC is 30 minutes.

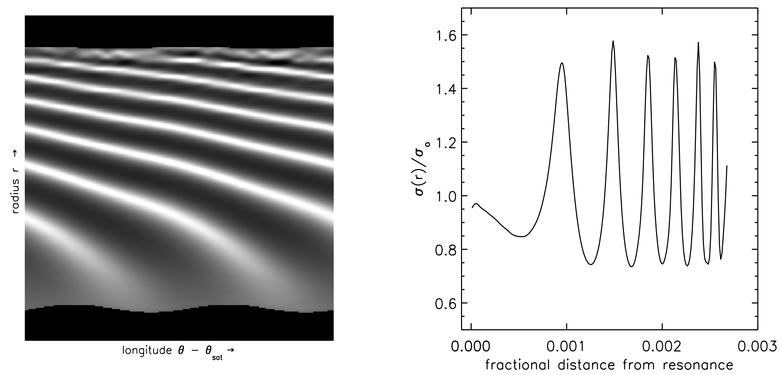

FIGURE 4: Simulation of an outward-propagating spiral density wave launched at an $m = 2$ ILR. Ring surface density $\sigma = 200$ gm/cm^2, $Q = 1.5$, and a compressible EOS is used. Drag with $C_d = 10^{-4}$ prevents the downstream waves from steepening so much that streamlines cross. Surface density crests trail in longitude as they advance in radius, so this is a trailing spiral. Note the peaks and troughs are not symmetric about $\sigma/\sigma_0 = 1$ (right), so this is a nonlinear spiral wave.

Main findings

- An Nbody method is successfully used to simulate collective phenomena in a planetary ring, such as the scalloping that occurs along the outer edge of Saturn's B ring, and the propagation of a spiral density wave in the ring's interior.
- The code uses streamline dynamics to calculate the ring's internal forces: gravity, pressure, and viscosity. This method is very effective at mitigating the particle-particle scattering that often prevents an Nbody code from resolving collective effects in a ring simulation.
- The purpose of the effort is to compare simulations to Cassini observations of the ring, to infer the ring's physical properties (surface density, equation of state, etc), and to test theories of ring evolution (such as the origin of the B ring's interesting $m <> 2$ modes).
- The next generation of this code will also track the ring's vertical displacements, which will then allow us to simulate the propagation of nonlinear spiral bending waves as well.

References

Borderies, Goldreich, Tremaine, 1985, Icarus, 63, 406.
Borderies, Goldreich, Tremaine, 1989, Icarus, 80, 344.
Hahn, Spitale, Porco, 2009, ApJ, 699, 686.
Longaretti & Borderies, 1991, Icarus, 94, 165.
Saha & Tremaine, 1992, AJ, 104, 1633.
Salo, 1995, Icarus, 117, 287.
Salo, Schmidt, Spahn, 2001, Icarus, 153, 295.
Spitale & Porco, 2010, AJ, in press. Wisdom & Holman, 1991, AJ, 102, 1528.